Dynamic Coupling Effects in Frictional Geomaterials—Stochastic Resonance

Yu-Hsing Wang[1] and J. Carlos Santamarina[2]

Abstract: Nonlinear, dynamic coupling effects and the manifestation of stochastic resonance are explored in the context of frictional geomaterials. The first experiment is designed to study a single interface between two mineral surfaces. Results demonstrate that as the amplitude of the driving signal approaches the threshold of static frictional resistance, the noise level required to cause slippage decreases and the peak output signal-to-noise ratio increases, inducing stochastic resonance. The second experimental study is conducted with sand specimens. While the classical signature of stochastic resonance is not observed in these multiinterface systems, nonlinear energy coupling effects appear. The effect of signal interaction through the nonlinear behavior of the medium is further studied by simultaneously exciting the specimen with two sinusoidal signals of different frequencies. The output response at the frequency of the primary driving signal increases as the amplitude of the secondary ''noise'' signal increases. Coupling increases as the driving signal brings the specimen to its nonlinear regime. The results highlight the interaction between friction and vibration in geomaterials, and suggest potential implications to experimental studies, construction operations, and dynamic phenomena such as seismic response and landslides.

DOI: 10.1061/(ASCE)1090-0241(2002)128:11(952)

CE Database keywords: Friction; Vibration; Noise; Resonance; Coupling; Seismic response.

Introduction

The shear strength in uncemented particulate materials and jointed rock masses is controlled by friction. Friction between mineral surfaces involves microscale phenomena such as adhesion, ploughing, debris interactions, asperity interactions, and deformation (Suh 1986; Hutchings 1992; Williams 1994; Bhushan et al. 1995). The resulting friction coefficient μ is not constant, but depends on sliding velocity, contact time, load, temperature, lubrication, and surface impurities among other variables (Dieterich 1978; Bowden and Tabor 1982; Rabinowicz 1992; Rymuza 1996). In addition, the shear force required to initiate sliding between two mineral surfaces is usually greater than the force required to maintain motion, that is, the static friction is greater than the kinetic friction, and stick–slip behavior can develop. Static friction establishes a threshold force in the nonlinear force-displacement behavior of frictional systems.

In particulate media, the angle of internal shear strength ϕ reflects the contributions of interparticle friction at contacts μ, particle rearrangement, dilation, particle crushing, and rotational frustration. The balance between these contributions is primarily controlled by void ratio and effective confining stress (Casagrande 1936; Taylor 1948; Bishop 1950). The macroscale stress–strain behavior for particulate media under cyclic loading is nonlinear. Fabric changes, volume contraction or dilation, nonlinearity, and energy losses become significant when the strain level γ exceeds the threshold strain γ_{th}. The theoretical value for the threshold strain for a cubic tetrahedral packing of spherical particles can be predicted, assuming Hertzian behavior (Santamarina et al. 2001):

$$\gamma_{th} = 1.4(\sigma/G)^{2/3} \tag{1}$$

where σ = applied effective confinement and G = shear modulus of particles. For sands at confining pressures ranging between 25 and 200 kPa, the measured threshold strain varies around $\gamma_{th} \approx 10^{-4}$ (see Dobry et al. 1982).

A system that experiences a frictional threshold may allow nonlinear dynamic coupling such as stochastic resonance. The purpose of this study is to explore these phenomena and to identify potential implications in geotechnical engineering.

Stochastic Resonance

Conventional stochastic resonance (SR) involves a nonlinear bistable system with a threshold barrier (which is analogous to a ball trying to roll between two valleys separated by a hill), a weak, periodic driving signal (incapable of forcing the ball to roll back and forth between the valleys, over the hill), and noise. Stochastic resonance takes place when the noise enhances the weak input signal, raising its intensity above the energy threshold of the nonlinear system (the ball rolls over the hill to the other valley).

The phenomenon was first postulated by Benzi et al. (1981) in the context of dynamic systems and soon afterwards applied to explain peaks in the spectrum of paleoclimatic records (Nicolis and Nicolis 1981; Benzi et al. 1982). Early experimental studies of stochastic resonance tested the Schmitt trigger circuit and laser-based systems (Moss 1994; Wiesenfeld and Moss 1995; Lanzara et al. 1997). More recently, the study of stochastic reso-

[1]Assistant Professor, Civil Engineering, Hong Kong Univ. of Science and Technology, Hong Kong.

[2]Professor, Civil and Environmental Engineering, Georgia Institute of Technology, Atlanta, GA 30332. E-mail: carlos@ce.gatech.edu

Note. Discussion open until April 1, 2003. Separate discussions must be submitted for individual papers. To extend the closing date by one month, a written request must be filed with the ASCE Managing Editor. The manuscript for this paper was submitted for review and possible publication on September 11, 2000; approved on January 8, 2002. This paper is part of the ***Journal of Geotechnical and Geoenvironmental Engineering***, Vol. 128, No. 11, November 1, 2002. ©ASCE, ISSN 1090-0241/2002/11-952–962/$8.00+$.50 per page.

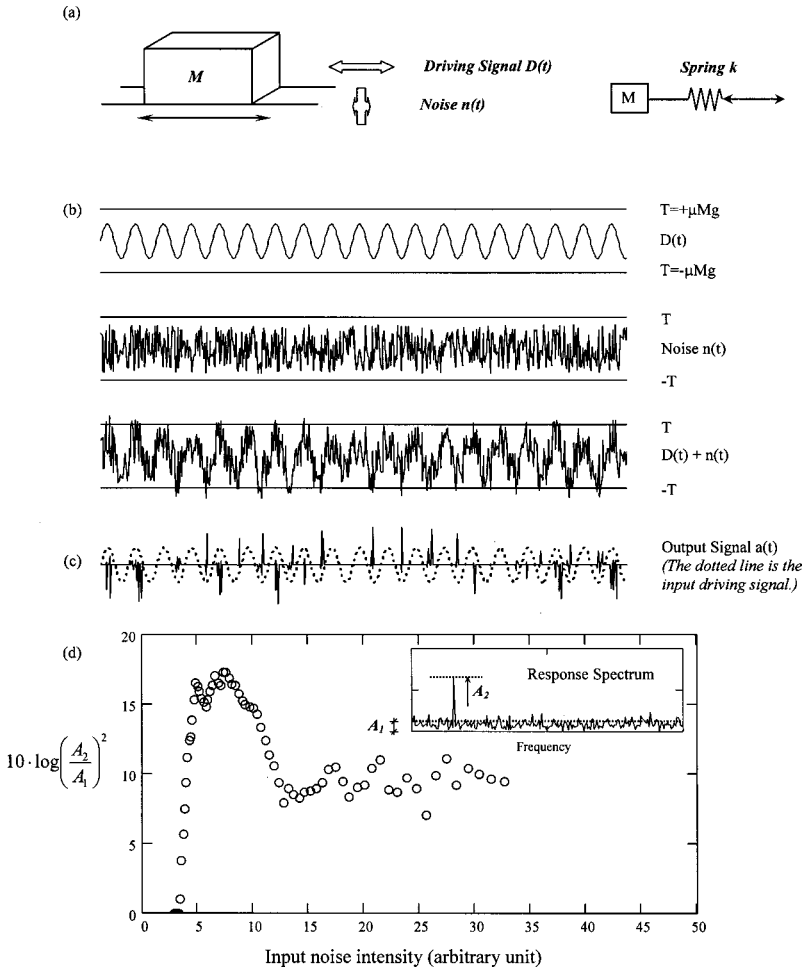

Fig. 1. Stochastic resonance; numerical simulation: (a) frictional system; (b) input driving signal (lower than static frictional threshold), noise, and total input signal; (c) output signal; and (d) output signal-to-noise ratio for different input noise intensities

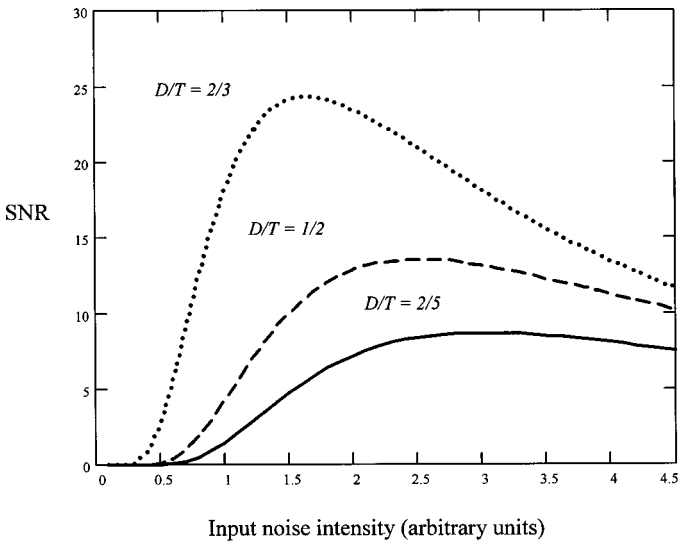

Fig. 2. Typical signature for stochastic resonance phenomena. Variation of output signal-to-noise ratio in bistable systems, according to Eq. (2).

nance or SR-like behavior has been extended to the analysis of biosystems, such as the integrate-and-fire model in sensory biology, sensory ability of neurons, and perception (Douglass et al. 1993; Collins et al. 1996; Cordo et al. 1996; Lipkin 1996; Raloff 1996; Jung and Wiesenfeld 1997).

In general, thermal agitation can be treated as input noise. Hence, SR may be responsible for errors in memory elements due to unwanted switching events, which result from a weak periodic signal aided by thermal noise (Torres and Trainor 1997). Likewise, SR can be used to explain the peak in thermally stimulated depolarization currents at certain temperatures (see the conductivity test results in Belarbi et al. 1997).

The effect of thermal agitation on friction at the atomic scale has been addressed using numerical simulations of atomic arrays (Braiman et al. 1999). SR-like behavior is observed in the numerical results by Tovstopyat-Nelip and Hentschel (2000), where noise is introduced as thermal agitation into a molecularly thin layer of a liquid lubricant. The effect of normal oscillations transverse to the shearing direction of the thin film between substrates has been experimentally studied (Heuberger et al. 1998) and further explored through molecular dynamics simulations (Gao et al. 1998). The results show that the normal oscillations prevent the ordering of molecules in the thin film (as in a stiff crystal), rendering ultralow friction. Stochastic resonance was not explored in these studies.

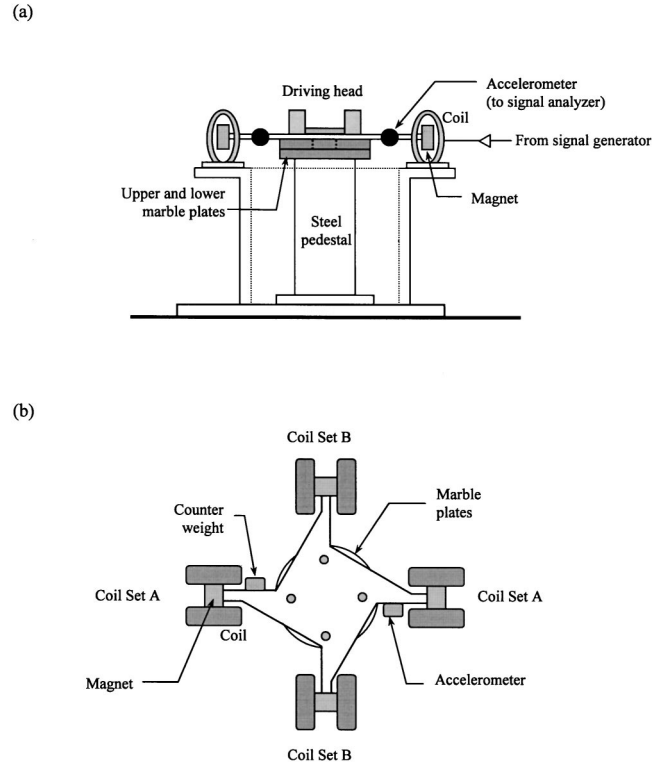

Fig. 3. Schematic diagram of experimental setup. Modified Stokoe resonant column. (a) Cross section and (b) plane view of the driving head.

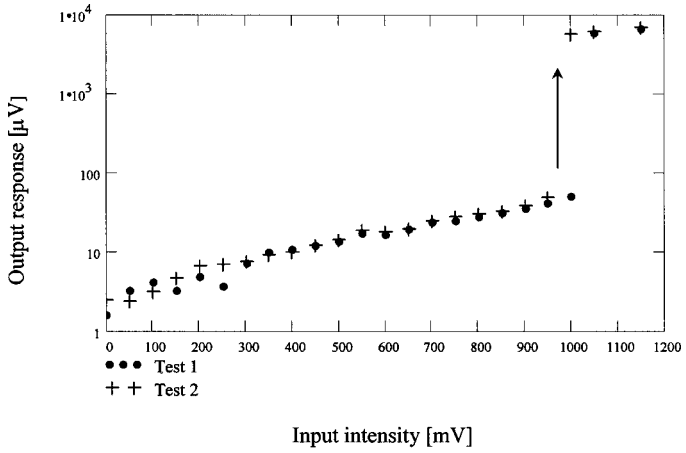

Fig. 4. Determination of frictional threshold for single interface (marble plates). Test is conducted by gradually increasing the amplitude of the input signal to coil set A (driving frequency $f_d = 16$ Hz—no noise).

Friction, Noise, and Stochastic Resonance at Engineering Scale

The phenomenon of stochastic resonance is herein explored within the context of a macroscale, engineering-type frictional system. Consider a mass M resting on a plane. The static friction force (or threshold) is $T = \mu M \cdot g$, where μ is the static friction coefficient and g is gravity. The system is numerically modeled as a spring with stiffness k, attached to a sliding mass M [Fig. 1(a)]. A cyclic lateral force $D(t) = D\sin(\omega t)$ is applied [Fig. 1(b)]. When the amplitude of the driving signal is lower than the threshold $|D(t)| < |T|$, the mass will not move. However, if noise $n(t)$ is added, the combined excitation $D(t) + n(t)$ may exceed the threshold T and make the mass move. The acceleration $a(t)$ experienced by the mass is shown in Fig. 1(c). Typically, the correlation between input and output is quantified by the output signal-to-noise ratio (SNR), which is the ratio between the spectral amplitude of the output signal at the frequency of the driving signal A_2 and the average spectral amplitude of the noise A_1, $\text{SNR} = 10\log(A_2/A_1)^2$. The results are plotted in Fig. 1(d) for different input noise levels. Fig. 1(d) shows the typical signature of

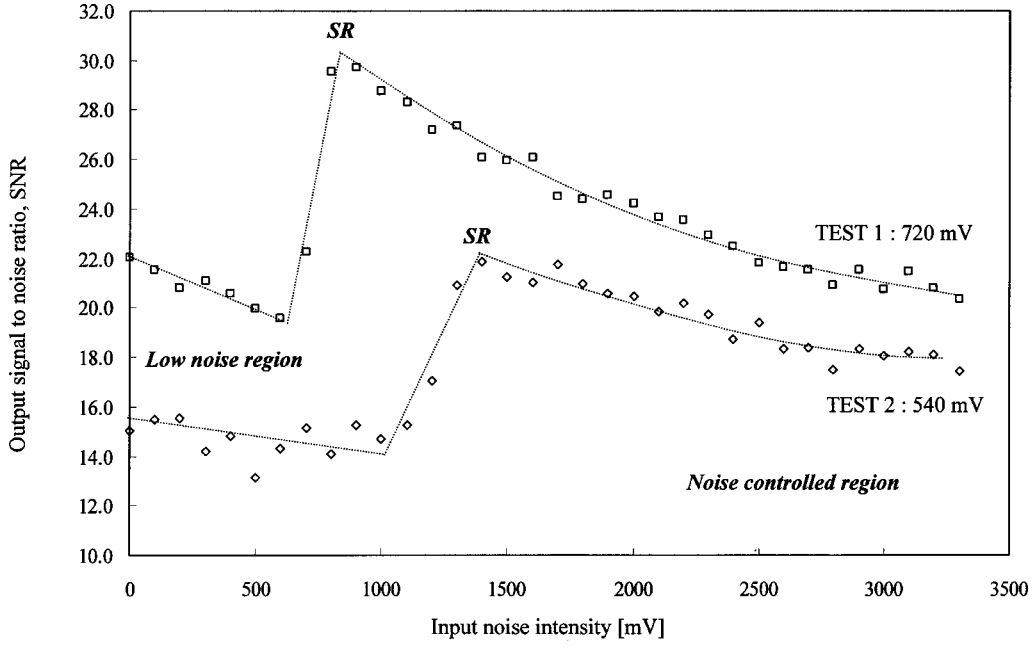

Fig. 5. Stochastic resonance in the single interface frictional system (marble plates). Two tests are shown for different amplitudes of the driving signal, 720 and 540 mV. The threshold for slippage without noise is about 1,000 mV (refer to Fig. 4).

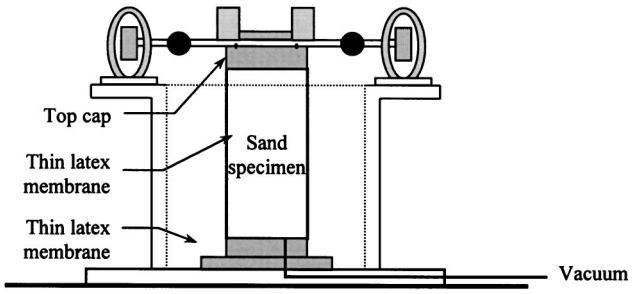

Fig. 6. Sand specimen test; schematic diagram of experimental setup

stochastic resonance, whereby the addition of noise causes a peak in the correlation between input and output at a certain optimal level of noise.

The output signal-to-noise ratio for stochastic resonance in a bistable potential can be approximated with the following equation (modified from Wiesenfeld and Moss 1995):

$$\mathrm{SNR} = 10 \log\left(\frac{A_2}{A_1}\right)^2 \propto \left[\frac{D(1-D/T)}{N/T}\right]^2 \exp\left(\frac{D/T-1}{N/T}\right) \qquad (2)$$

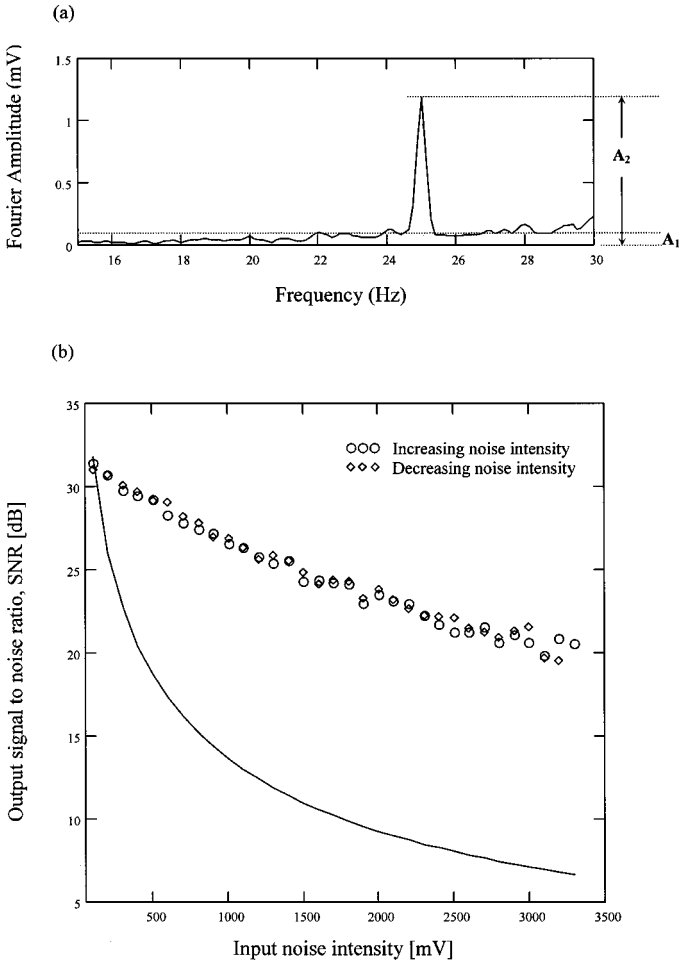

Fig. 7. SR test in sand specimen (Ottawa sand 20–30). Resonant frequency is 116 Hz; driving signal frequency is fixed at $f_d = 25$ Hz. (a) Typical response spectrum for a selected noise level A_1. (b) SNR versus input noise intensity. Solid line is the predicted signal-to-noise ratio for a linear system.

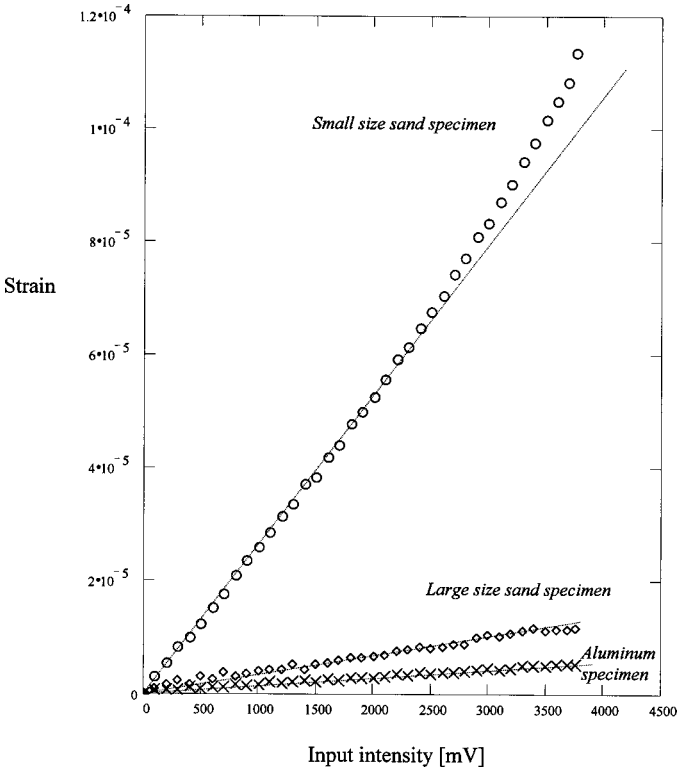

Fig. 8. Load-deformation behavior for sand and aluminum specimens. Tests run at $f_d = 32$ Hz (no noise).

where A_2 = ratio between the spectral density of the output signal at the driving frequency f_d, A_1 = response spectral density due to noise, D = amplitude of the driving signal, and N = amplitude of the input noise. Fig. 2 shows stochastic resonance signatures computed with Eq. (2). The closer the amplitude of the driving signal intensity D to the threshold level T, the lower the noise intensity N required to overcome the threshold, and the higher the peak signal-to-noise ratio.

Experimental Study with Marble Plates (Single Interface)

The device used in this study to assess nonlinear dynamic effects and stochastic resonance in geomaterials is based on the four coil-magnet driving head used in the Stokoe resonant column (Fig. 3). The electrical signal fed to the coils fixed to the external frame causes a magnetic field that interacts with the magnets attached to the specimen. In this first study, the specimen consists of two annular marble plates. The upper plate is connected to the driving head that contains the magnets. The lower marble plate is anchored to the steel pedestal. The four driving coils of the driving head are connected in two separate sets. One set is used to apply the driving sinusoidal signal $D(t)$ and the other set of coils is used to input the noise signal $n(t)$; therefore, signal and noise are colinear (rather than transverse to each other). The two input signals are generated by separate signal generators. The rotation of the driving head is monitored with an accelerometer that is connected to a signal analyzer.

The surface roughness for the two marble plates is determined with a profilometer (model Talysurf series 2; resolution $\Delta z = \Delta x = 0.2$ μm). The main length scale for the surface roughness is 35.3 μm, with an average amplitude of 0.49 μm. A thin coat of

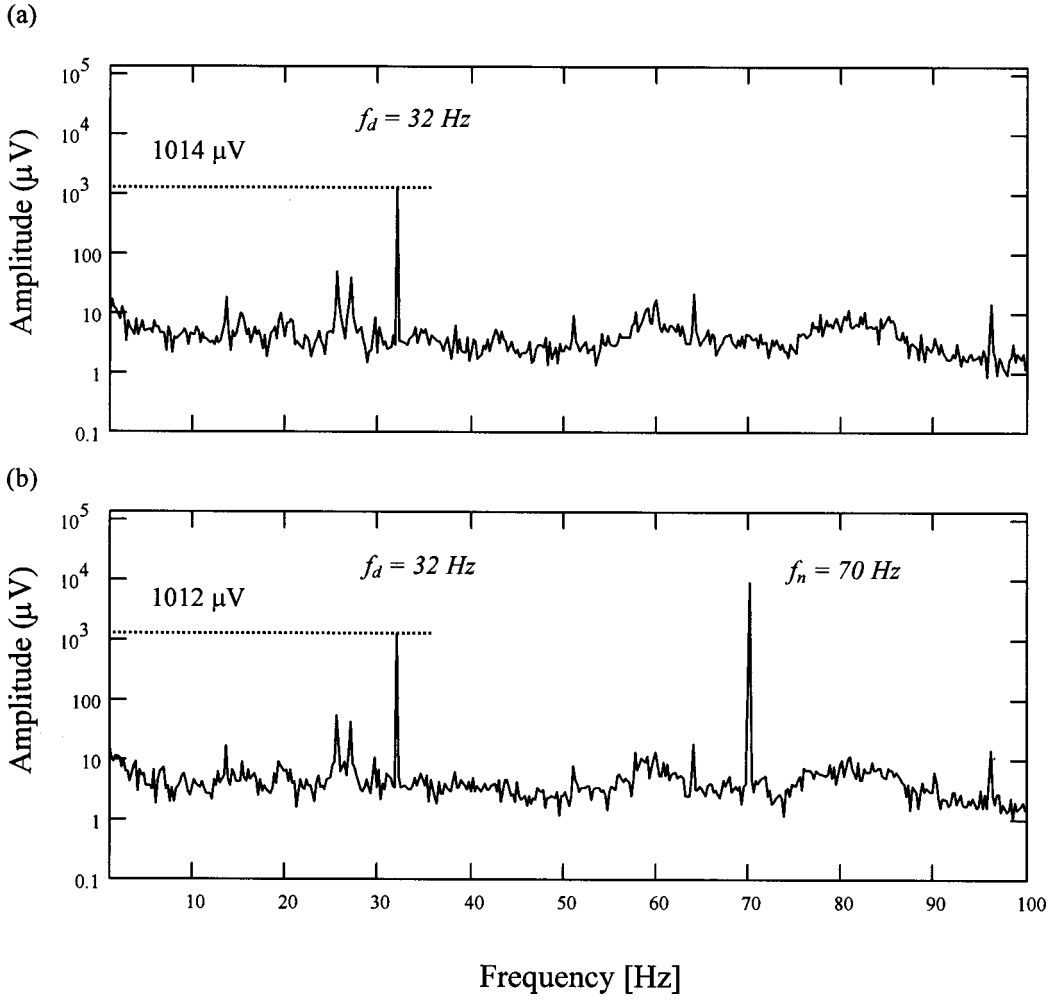

Fig. 9. Spectral response for aluminum specimen. (a) Only $f_d = 32$ Hz signal is applied. (b) $f_n = 70$ Hz signal is added, in this case at its maximum amplitude (4,263 mV).

talc powder is applied onto the surfaces to reduce interfacial static friction so that the driving head is capable of moving the marble plate.

The friction threshold is determined using the coil–magnet actuators, gradually increasing the amplitude of the driving sinusoidal signal at a frequency $f_d = 16$ Hz. The recorded output response is plotted versus the amplitude of the input signal in Fig. 4 (at $f_d = 16$ Hz). The frictional threshold corresponds to the input intensity when the marble plate begins moving and causes a sharp increase in the output. The pseudolinear increase observed in the response at low input intensity reflects the linear torsional deformation of the specimen and steel pedestal.

The test for nonlinear coupling is also run with the $f_d = 16$ Hz driving signal (coil set A). While the amplitude of the driving signal is fixed below the measured threshold, the amplitude of the noise signal fed to coil set B is gradually increased from 0 to 3,300 mV, in 100 mV increments (noise is band limited from 1 to 26 Hz). The signal-to-noise ratio in the measured output signal (at $f_d = 16$ Hz) is recorded for each level of input noise (four records are stacked in each case). A plot of the output signal-to-noise ratio versus the input noise intensity is presented in Fig. 5. In this case, the output signal-to-noise ratio is the ratio between the spectral density of the output signal and the average noise background at the driving frequency $f_d = 16$ Hz. The results are shown for two tests run with different amplitudes of the sinusoidal signal (720 and 540 mV; both at $f_d = 16$ Hz). The results show three stages (Fig. 5, refer to Fig. 2 for comparison):

Stage 1: Low-Noise, Linear System

The response at 16 Hz cannot be distinguished from the background noise. There is no slippage at the marble–talc–marble interface, and the response is controlled by the linear behavior of the specimen–pedestal system; thus, the signal-to-noise ratio decreases as the input noise intensity increases.

Stage 2: Stochastic Resonance Stochastic Resonance

As the amplitude of the noise is increased further, the marble plate begins moving and the output signal-to-noise ratio increases sharply; that is, the noise enhances the driving signal above the frictional threshold *T*, and the marble plate moves coherently with the driving signal.

Stage 3: High, Noise-Controlled Response

As the input noise intensity is further increased, the response becomes noise controlled, and the output signal-to-noise ratio gradually decreases. Note that the driving signal with higher amplitude *D* needs lower noise intensity to overcome the threshold,

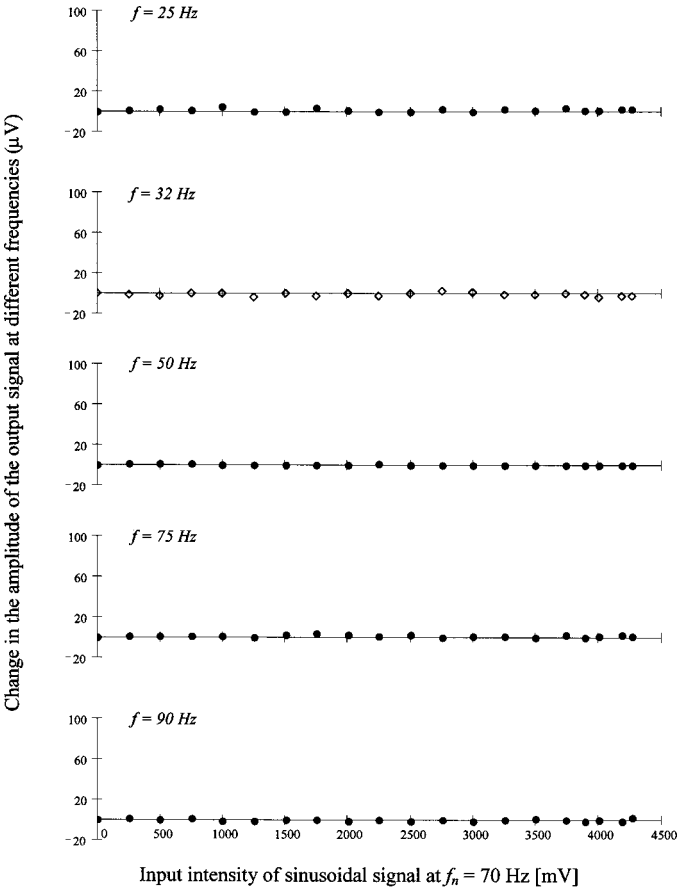

Fig. 10. Aluminum specimen. Change in amplitude of output at different frequencies. Driving signal $f_d = 32$ Hz is kept at a constant peak-to-peak amplitude (3384 mV). Amplitude of the $f_n = 70$ Hz signal is increased from 0 to 4263 mV. Note: compare the vertical scale to the one used in Fig. 14.

and the value of the signal-to-noise ratio is larger (Fig. 2). The results shown in Fig. 5 are characteristic stochastic resonance signatures. The study was repeated for other excitation frequencies and interfacial conditions and reached similar conclusions.

Experimental Study with Sand (Multiple Interfaces)

Does stochastic resonance manifest in a system with a large number of frictional interfaces such as a soil mass? The following sequence of experimental studies explores this question, and evaluates energy coupling between excitations at different frequencies when the soil mass is at the verge of nonlinearity.

Testing for Stochastic Resonance

A standard resonant column specimen is prepared with Ottawa sand 20–30 (mean particle diameter $D_{50} = 0.72$ mm, coefficient of uniformity $C_u = 1.19$, specimen height $H_1 = 14.22$ cm, and specimen diameter $D_1 = 7.11$ cm). The test is run with the same coil configuration used with the marble specimen, that is, colinear driving and noise signals. The cylindrical specimen is contained within two metal caps and a very thin latex membrane (Fig. 6). The driving head is fixed to the top cap, and the bottom cap is anchored to the base. Confinement is applied by internal vacuum 46 kPa. Note that the test is purposely run at $f_d = 25$ Hz, far from the system resonance ($f_r = 116$ Hz).

A typical spectral response at a selected noise level is shown in Fig. 7(a). The ratio A_2/A_1 is plotted versus the amplitude of the input noise N in Fig. 7(b). There is no indication of stochastic resonance in this response. The ratio A_2/A_1 in a linear system is

$$\frac{A_2}{A_1} = \frac{H(D+N)}{H(N)} = 1 + \frac{D}{N} \tag{3}$$

where D = amplitude of the driving signal; N = amplitude of the input noise; and H = frequency response of the system. Eq. (3) is plotted in Fig. 7(b) as well. It can be concluded that while the system does not manifest stochastic resonance (that is, a peak response at some optimal noise level), the nonlinear coupling between the driving signal and the noise causes a response higher than that expected for a linear system.

Nonlinear Energy Coupling

An additional study is implemented to further assess nonlinear coupling in soils. Two specimens with different geometry are tested (diameter $D_1 = 7.11$ cm, height $H_1 = 14.22$ cm; $D_2 = 3.57$ cm, $H_2 = 7.1$ cm). Both specimens are prepared with Ottawa sand 20–30, and are subjected to vacuum pressure ($\sigma_{conf} = 46$ kPa). A hollow aluminum specimen is also tested to obtain the response of a linear elastic system for comparison (outside diameter 2.54 cm; inside diameter 2.354 cm; height 13.94 cm). The resonant frequencies for the aluminum specimen, and the large and the small sand specimens are 123, 116.5, and 54.5 Hz, respectively. The load-deformation response of each specimen is determined first. Then, the nonlinear coupling is explored.

Load-Deformation Response

The load deformation for each specimen is determined at frequency $f_d = 32$ Hz, without noise (coil set A only), and is shown in Fig. 8. The volume average strain level at peak rotation can be computed from the measured acceleration as

$$\gamma = \frac{0.8\ R\ \text{acc}}{dl\omega^2} \tag{4}$$

where R = radius of the specimen; d = distance between the center of the specimen and the position of the accelerometer; l = height of the specimen; ω = angular frequency; and acc = peak acceleration determined from the output record (the accelerometer response is 100 mV for 1 g). Because the cylindrical specimen is subjected to torsional deformation, the shear strain is not uniformly distributed along the radial direction; the factor 0.8 in Eq. (4) is used to estimate the representative volume average strain (Cascante et al. 1998).

The aluminum and the large sand specimens show approximate linear behavior within the tested range. The small diameter sand specimen deviates from linearity at large strains. Clearly, there is no sudden macroscale slippage, even though strains γ exceed the threshold strain γ_{th}, and fabric changes and slippage at contacts are expected.

Energy Coupling Effects

The evaluation of nonlinear energy coupling is implemented by imposing two sinusoidal signals: the driving signal is fixed at $f_d = 32$ Hz (coil set A), and the "noise signal" is modeled as another

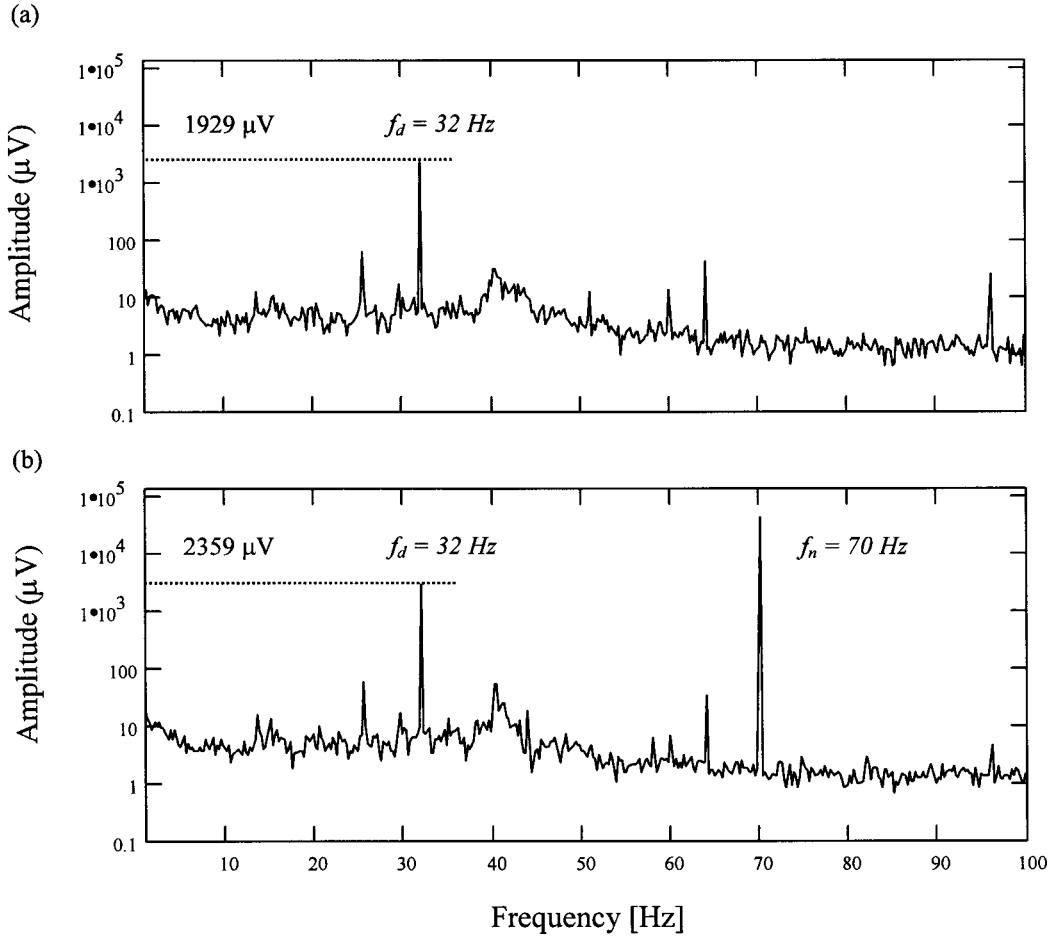

Fig. 11. Spectral response for small-size sand specimen. (a) Only $f_d = 32$ Hz signal is applied. (b) $f_n = 70$ Hz signal is added, in this case at its maximum amplitude (4263 mV).

colinear sinusoidal signal at $f_n = 70$ Hz (coil set B). The intensity of the $f_n = 70$ Hz sinusoidal signal is gradually increased and the output response at 32 Hz is recorded in each case.

The results obtained with the linearly elastic aluminum specimen confirm the absence of coupling in a linear system, as shown in Figs. 9 and 10. Fig. 9 shows the spectral response without the "noise" signal ($f_n = 70$ Hz) and for maximum amplitude of the noise signal. Fig. 10 shows a summary plot of the response at selected frequencies for different amplitudes of the $f_n = 70$ Hz signal. The output response at all frequencies remains constant (including at $f_d = 32$ Hz) while the intensity of the $f_n = 70$ Hz sinusoidal signal increases, the expected response for a linear system.

On the other hand, Figs. 11 and 12 show parallel test results for the small-size sand specimen. Fig. 12 clearly shows that the response at $f_d = 32$ Hz increases as the amplitude of the 70 Hz noise signal increases. Furthermore, the output of the response is amplified at the frequency of the driving signal, $f_d = 32$ Hz, only.

The interplay between the amplitudes of the two signals in the small-size sand specimen is studied in detail by systematically and independently varying the amplitude of both signals. When the amplitude of the driving signal ($f_d = 32$) is 1,816 mV or higher, the strain level in the specimen exceeds the threshold strain γ_{th}, even if the amplitude of the $f_n = 70$ signal is null (Fig. 8). The results shown in Fig. 13 indicate that the amplitude of the response at 32 Hz is clearly affected by the amplitude of the $f_n = 70$ Hz, in particular, when the amplitude of driving signal is sufficient to bring the specimen to its nonlinear regime ($\gamma > \gamma_{th}$).

The results obtained and observations made with the large-size specimen are similar to those presented in Figs. 11–13. However, coupling effects are less pronounced, in agreement with the lower strain level that is produced in the larger diameter specimen.

Interplay between Harmonics—Simulation

A numerical simulation is conducted to facilitate the interpretation of results obtained when two single frequency sinusoids are simultaneously applied onto a nonlinear system. Concepts related to the development of harmonics in nonlinear response and the characteristics of beat signals are reviewed first.

Preliminary Concepts

Consider a nonlinear thresholding system being excited with a single frequency sinusoid $x(t)$ of frequency f. The system response $y(t)$ is an "altered sinusoid" of the same global periodicity as the input signal. The Fourier transform of a signal is fitting the signal with a Fourier series. While the discrete Fourier transform of the input is a spike at frequency f, the Fourier transform

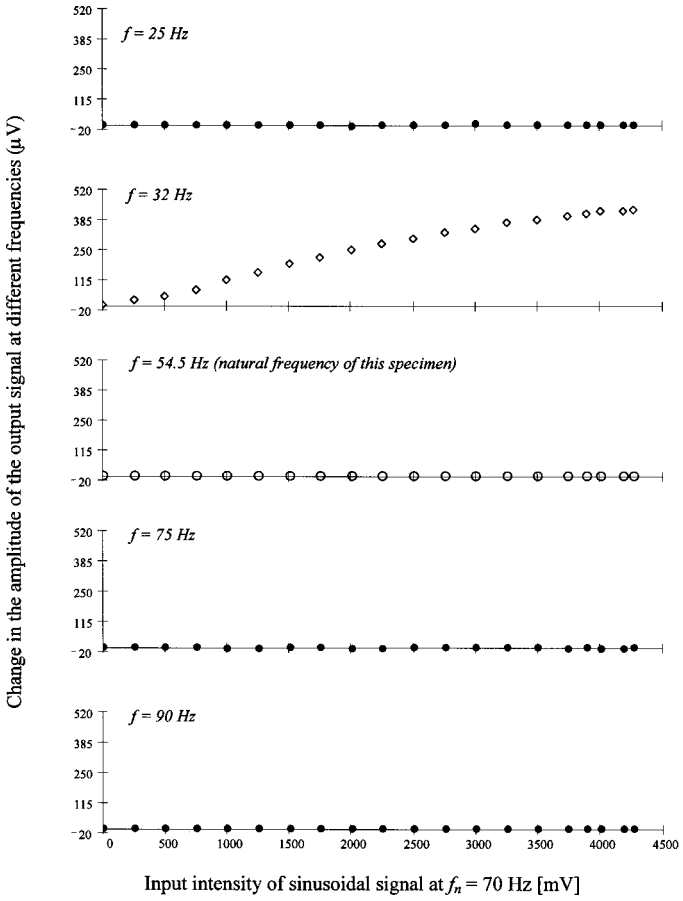

Fig. 12. Small-size sand specimen. Change in amplitude of output at different frequencies (selected to avoid harmonics and beat effects—refer to Fig. 15). Driving signal $f_d = 32$ Hz is kept at a constant peak-to-peak amplitude (761 mV). Amplitude of the $f_n = 70$ Hz signal is increased from 0 mV to 4263 mV. Note: compare the vertical scale to the one used in Fig. 10.

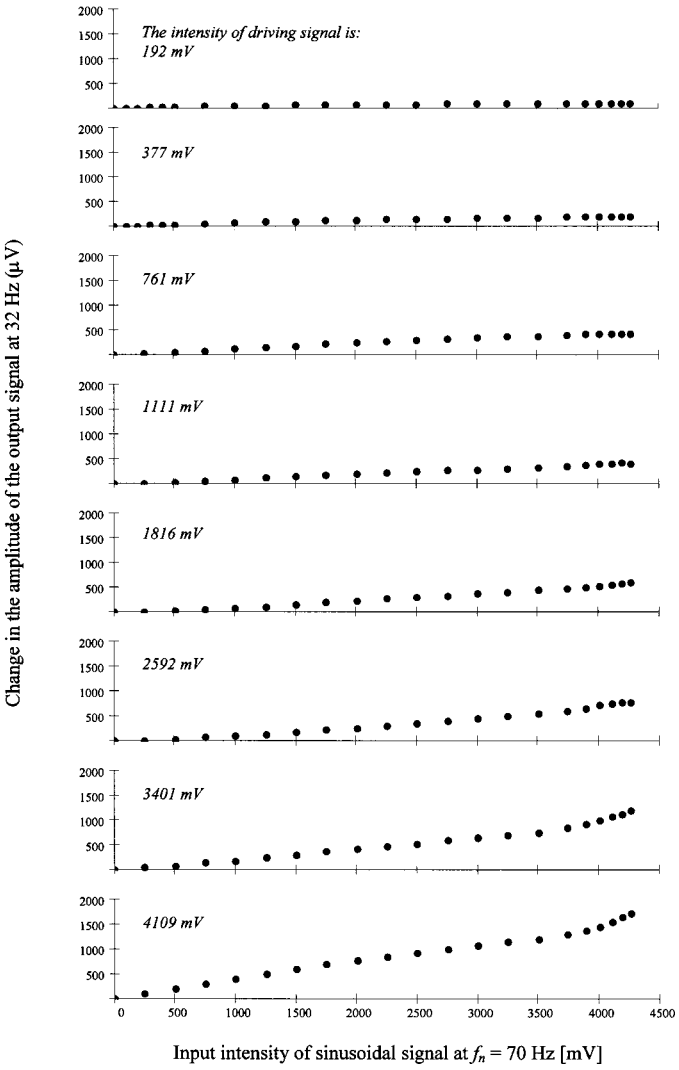

Fig. 13. Small-size sand specimen. Change in amplitude of output signal at 32 Hz for different amplitudes of the $f_n = 70$ Hz input signal. Each trace was obtained for different amplitudes of $f_d = 32$ Hz input signal.

of the response shows energy not only at the frequency *f*, but also in the higher harmonics, *nf*, which are needed to properly fit the periodic signal $y(t)$.

On the other hand, the superposition of two single frequency sinusoids $x_1(t)$ and $x_2(t)$ of frequencies f_1 and f_2 renders a signal with beats, i.e., periodic variations in amplitude. The frequency of these beats is $\Delta f = |f_1 - f_2|$. When a linear system is subjected to $x_1(t) + x_2(t)$, the response is also a beat signal, and the discrete Fourier transform of the response shows energy at frequencies f_1 and f_2 only.

Nonlinear Coupling—Simulation

Then, what is the spectral response of a nonlinear thresholding system subjected to the combined signals $x_1(t) + x_2(t)$? Given that the input is maximum at the peak of the beats, the maximum response should develop with the periodicity of the beats. Furthermore, higher harmonics are expected in relation to the input frequencies f_1 and f_2, as discussed earlier. Indeed, numerical simulations by time integration confirm that energy peaks are expected at frequencies

$$pf_1 + qf_2 \pm r(f_1 - f_2) \tag{5}$$

where *p*, *q*, and $r = 0,1,2$, etc. A numerical example is presented in Fig. 14. Fig. 14 shows the following: the time series for the combined input signals ($f_1 = 32$ Hz, $f_2 = 70$ Hz) with periodic peaks or beats; the simulated output obtained by thresholding; the discrete Fourier transform of the input signal with peaks only at f_1 and f_2; and the discrete Fourier transform of the output showing peaks at frequencies predicted by Eq. (5). Careful observation of Fig. 11 shows minor effects at the predicted frequencies (a low level of nonlinearity is produced in this case—stored records are limited to 100 Hz).

Implications in Geomechanics

From a microscale perspective, confined dense particulate materials inherently display an energy threshold, even in the absence of friction. Consider the packing of particles shown in Fig. 15. If these particles are subjected to shear, energy will be needed to distort the packing from one stable state to the next stable state.

While the experiments with soils did not show the development of stochastic resonance, the study is limited to colinear noise and driving signals. Therefore, the development of SR in soils is not formally falsified by this study. In particular, transverse exci-

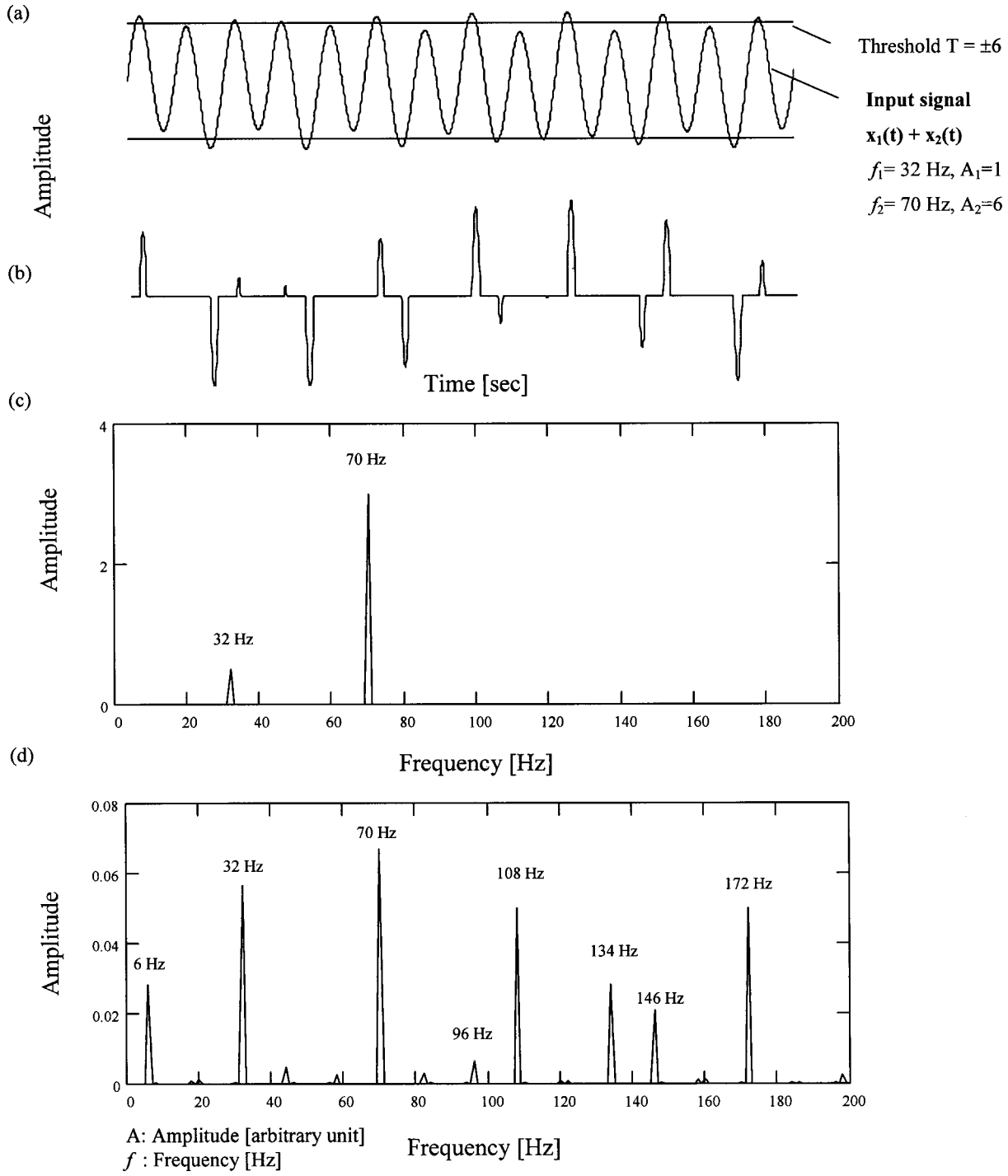

Fig. 14. Interplay between harmonics and beat frequency; numerical simulation. (a) Total input signal. System threshold set at $T = \pm 6$. (b) Simulated response of nonlinear thresholding system. (c) Fourier spectrum of input signal; peaks only appear at f_1 and f_2. (d) Fourier spectrum of simulated response; peaks occur at frequencies predicted by Eq. (5).

tation should be explored, such as a sand column subjected to random vertical vibrations while a weak transverse oscillation is applied (significant resonant-type reductions in frictional resistance have been observed in transverse vibration experiments with sliders—Tolstoi 1967; Kudinov and Tolstoi 2001). In addition, lightly cemented soils localize during shear rendering a structure similar to the marble plates; therefore, they may also experience SR response.

Vibration and micropulses at the level of surface asperities was postulated within the asperity theory of friction to explain the reduction from static to kinetic friction (reviews by Isbrahim 1994a,b, and by Feeny et al. 1998). Furthermore, vibration at the particle level in granular materials can lead to its fluidization, for example, when a layer of sand is placed on a vibrating plate (Umbanhowar 1997; Umbanhowar and Swinney 2000; Duran 2000). Hence, the friction coefficient can be effectively lowered by fluidization (Zik et al. 1992). Note that fluidization resembles thermal agitation at the molecular level; thus, observations from atomic scale studies reviewed earlier in this paper are relevant, including the potential development of stochastic resonance.

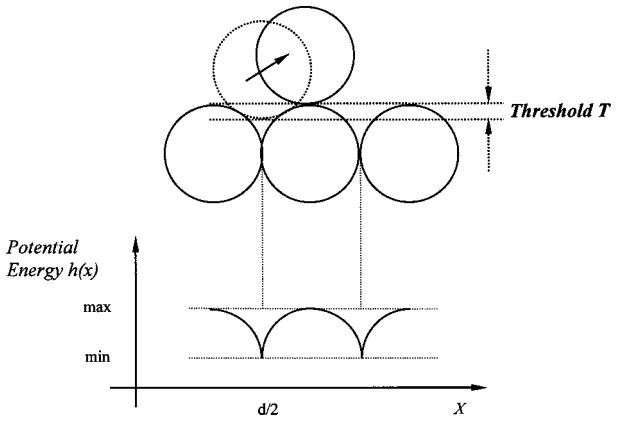

Fig. 15. Shear deformation of particulate materials experiences an energy threshold even in the absence of interparticle friction.

These results and observations suggest that the enhanced understanding of nonlinear dynamic energy coupling effects in geomaterials are important to the control of friction in geomechanics, to the assessment of dynamic events, and to the potential development of improved construction operations. Examples include:

Displacement of Slopes during Seismic Excitation

In seismic excitation, multiple frequencies accompany the predominant frequency; hence, frictional systems such as soils and fractured rocks may experience nonlinear coupling between the prevailing frequency in the seismic event and the energy in the sideband frequencies. This may increase the displacement of slopes during earthquakes (refer to the block model analysis in Ambraseys and Menu 1988). Alternatively, the seismic energy can be considered as the noise that is superimposed onto the internal cyclic motion of creeping slopes (R. F. Scott, personal communication, 1987).

Seismic Site Response and Amplification

Similar to the previous discussion, energy in frequencies outside the natural frequency of the soil formation can couple nonlinearly and magnify the site response. In particular, the interaction between the simultaneous vertical and transverse excitation during earthquakes requires further analysis.

Landslides

Sliding can generate its own noise to sustain the motion. The phenomenon of ''acoustic fluidization'' was proposed by Melosh, and used to explain the large distance traveled by some landslides, the dynamical weakening of faults, and large impact crater formation (Melosh 1986, 1996; Ivanov 1998—discussion in Sornette and Sornette 2000).

Interpretation of Experimental Studies

Nonlinear coupling effects need to be taken into consideration while interpreting the dynamic response of soils or fractured rocks observed in experimental studies. Potentially, negative damping could be inferred if the effect of noise or a second signal is not recognized.

Improvement in Field Procedures

Improvement in field procedures including petroleum reservoir stimulation by vibration, vibratory pile driving, and vibratory soil densification.

Conclusions

1. Atomistic and engineering scale observations show that friction and vibration are interrelated: while friction causes vibrations, vibrations affect friction.
2. Stochastic resonance can take place in frictional systems. The behavior is similar to phenomena observed in other nonlinear systems with an energy threshold. When the amplitude of the driving signal approaches the threshold of frictional resistance, the noise level required to cause slippage decreases and the peak output signal-to-noise ratio increases.
3. Nonlinear dynamic coupling is readily observed in sand specimens when the system is excited with two colinear sinusoidal signals of different frequencies. The output response at the frequency of the primary driving signal increases as the amplitude of the secondary signal increases. Coupling increases as the driving signal brings the specimen to its nonlinear regime, $\gamma > \gamma_{th}$. The classical signature of stochastic resonance is not manifested in multi-interface sand specimens when the signal and the noise are colinear. A similar study should be repeated to investigate the coupling between simultaneous transverse excitations in soils.
4. Nonlinear coupling alters the energy content in the harmonics of the input signals and of the beat frequency.
5. Proper understanding of nonlinear dynamic energy coupling effects in frictional geomaterials can lead to the enhanced control of friction, improved analyses of dynamic events, and further developments in construction operations.

Acknowledgments

This research was conducted by the writers at the Georgia Institute of Technology, and was supported by a grant from the National Science Foundation. The writers are grateful to Dr. M. Geilikman for bringing the phenomenon of stochastic resonance to our attention. Dr. J. Dove characterized the surface of the marble specimen.

References

Ambraseys, N. N., and Menu, J. M. (1988). ''Earthquake-induced ground displacements.'' *Earthquake Eng. Struct. Dyn.,* 16, 985–1006.

Belarbi, H., Haouzi, A., Giuntini, J. C., Zanchetta, J. V., Niezette, J., and Vanderschueren, J. (1997). ''Interpretation of orientation polarization in homoionic dry montmorillonite.'' *Clay Miner.,* 32, 13–20.

Benzi, R., Parisi, G., Sutera, A., and Vulpiani, A. (1982).''Stochastic resonance in climatic change.'' *Tellus,* 34, 10–16.

Benzi, R., Sutera, A., and Vulpiani, A. (1981). ''The mechanism of stochastic resonance.'' *J. Phys. A,* 14, L453–L457.

Bhushan, B., Israelachvili, J. N., and Landman, U. (1995). ''Nanotribology: Friction, wear, and lubrication at the atomic scale.'' *Nature (London),* 374, 607–616.

Bishop, A. W. (1950). ''Discussion to 'Measurement of the shear strength of soils' by Skempton and Bishop.'' *Géotechnique,* 36, 65–78.

Bowden, F. P., and Tabor, D. (1982). *Friction—An introduction to tribology,* Reprint Ed., Krieger, New York.

Braiman, Y., Hentschel, H. G. E., Family, F., Mak, C., and Krim, J. (1999). ''Tuning friction with noise and disorder.'' *Phys. Rev. E,* 59, R4737–R4740.

Casagrande, A. (1936). ''Characteristics of cohesionless soils affecting the stability of slopes and earth fills.'' *J. Boston Society of Civil Engineers*, January; reprinted in *Contributions to soil mechanics (1925–1940)*, the Boston Society of Civil Engineers, 1948, 257–276.

Cascante, G., Santamarina, J. C., and Yassir, N. (1998). ''Flexural excitation in a standard torsional–resonant column device.'' *Can. Geotech. J.*, 35, 478–490.

Collins, J. J., Imhoff, T. T., and Grigg, P. (1996). ''Noise-enhanced tactile sensation.'' *Nature (London)*, 383, 770–770.

Cordo, P., Inglis, J. T., Verschueren, S., Collins, J. J., Merfeld, D. M., Rosenblum, S., Buckley, S., and Moss, F. (1996). ''Noise in human muscle spindles.'' *Nature (London)*, 383, 769–770.

Dieterich, J. H. (1978). ''Time-dependent friction and the mechanics of stick–slip.'' *Pure Appl. Geophys.*, 116, 790–806.

Dobry, R., Ladd, R. S., Yokel, F. Y., Chung, R. M., and Powell, D. (1982). *Prediction of pore water pressure buildup and liquefaction of sands during earthquakes by the cyclic strain method*, National Bureau of Standards Building Science Series 138, U.S. Government Printing Office, Washington, D.C.

Douglass, J. K., Wilkens, L., Pantazelou, E., and Moss, F. (1993). ''Noise enhancement of information transfer in crayfish mechanoreceptors by stochastic resonance.'' *Nature (London)*, 365, 337–340.

Duran, J. (2000). *Sands, powders, and grains—An introduction to the physics of granular materials*, Springer, New York.

Feeny, B., Guran, A., Hinrichs, N., and Popp, K. (1998). ''A historical review on dry friction and stick–slip phenomena.'' *Appl. Mech. Rev.*, 51, 321–341.

Gao, J., Luedtke, W. D., and Landman, U. (1998). ''Friction control in thin-film lubrication.'' *J. Phys. Chem. B*, 102, 5033–5037.

Heuberger, M., Drummond, C., and Israelachvili, J. (1998). ''Coupling of normal and transverse motions during friction sliding.'' *J. Phys. Chem. B*, 102, 5038–5041.

Hutchings, I. M. (1992). *Tribology: friction and wear of engineering materials*, CRC, Ann Arbor, Mich.

Isbrahim, R. A. (1994a). ''Friction-induced vibration, chatter, squeal, and chaos. Part I: Mechanics of contact and friction.'' *Appl. Mech. Rev.*, 47, 209–226.

Isbrahim, R. A. (1994b). ''Friction-induced vibration, chatter, squeal, and chaos. Part II: Dynamics and modeling.'' *Appl. Mech. Rev.*, 47, 227–253.

Ivanov, B. A. (1998). ''Large impact crater formation: Thermal softening and acoustic fluidization.'' *Meteoritics Planetary Sci.*, 33, A76.

Jung, P., and Wiesenfeld, K. (1997). ''Too quiet to hear a whisper.'' *Nature (London)*, 385, 291–291.

Kudinov, N. V., and Tolstoi, D. M. (2001). ''Friction and oscillations.'' *Tribology—Lubrication, friction, and wear*, I. V. Kragelsky and V. V. Alisin, eds., Professional Engineering, 473–489.

Lanzara, E., Mantegna, R. N., Spagnolo, B., and Zangara, R. (1997). ''Experimental study of a nonlinear system in the presence of noise: The stochastic resonance.'' *Am. J. Phys.*, 65, 341–349.

Lipkin, R. (1996). ''Digital noise sharpens vague image.'' *Sci. News (Washington, D. C.)*, 149, 196–196.

Melosh, H. J. (1986). ''The physics of very large landslides.'' *Acta Mech.*, 64, 89–99.

Melosh, H. J. (1996). ''Dynamical weakening of faults by acoustic fluidization.'' *Nature (London)*, 379, 601–606.

Moss, F. (1994). ''Stochastic resonance: From the ice ages to the monkey's ear.'' *Contemporary problems in statistical physics*, G. H. Weiss, ed., Society for Industrial and Applied Mathematics, 205–253.

Nicolis, C., and Nicolis, G. (1981). ''Stochastic aspects of climatic transitions—Additive fluctuations.'' *Tellus*, 33, 325–234.

Rabinowicz, E. (1992). ''Friction fluctuations.'' *Fundamentals of friction: macroscopic, and microscopic processes*, I. L. Signer, and H. M. Pollock, eds., Kluwer Academic, Dordrecht, The Netherlands, 25–34.

Raloff, J. (1996). ''Is noise a neural necessity?'' *Sci. News (Washington, D. C.)*, 150, 330–331.

Rymuza, Z. (1996). ''Energy concept of the coefficient of friction.'' *Wear*, 199, 187–196.

Santamarina, J. C., Klein, K., and Fam, M. (2001). *Soils and waves*, Wiley, New York.

Sornette, D., and Sornette, A. (2000). ''Acoustic fluidization for earthquakes?'' *Bull. Seismol. Soc. Am.*, 90, 781–785.

Suh, N. P. (1986). *Tribophysics*, Prentice-Hall, Englewood Cliffs, N.J.

Taylor, D. (1948). *Fundamentals of soil mechanics*, Wiley, New York.

Tolstoi, D. M. (1967). ''Significance of the normal degree of freedom and natural normal vibrations in contact friction.'' *Wear*, 10, 199–213.

Torres, J. L., and Trainor, L. (1997). ''Stochastic resonance and computation.'' *J. Appl. Phys.*, 82, 2702–2703.

Tovstopyat-Nelip, I., and Hentschel, H. G. E. (2000). ''Friction and noise-induced coherent structures in boundary lubrication.'' *Phys. Rev. E*, 61, 3318–3324.

Umbanhowar, P. B. (1997). ''Patterns in the sands.'' *Nature (London)*, 389, 541–542.

Umbanhowar, P. B., and Swinney, H. L. (2000). ''Wavelength scaling and square/stripe and grain mobility transitions in vertically oscillated granular layers.'' *Physica A*, 288, 344–362.

Wiesenfeld, K., and Moss, F. (1995). ''Stochastic resonance and the benefits of noise—From ice ages to crayfish and SQUIDs.'' *Nature (London)*, 373, 33–36.

Williams, J. A. (1994). *Engineering tribology*, Oxford Science, New York.

Zik, O., Stavans, J., and Rabin, Y. (1992). ''Mobility of a sphere in vibrated granular media.'' *Europhys. Lett.*, 17, 315–319.